Anomalous Heat Generation during Hydrogenation of Carbon (Phenanthrene)

Tadahiko Mizuno[1] and Shigemi Sawada[2]
[1] *Graduate School of Engineering, Hokkaido University*
Division of Energy Environment
Kita-ku Kita 13 Nishi 8, Sapporo 060-8628, Japan
[2] *Sequence Co. Ltd, Yamanote 1-22-11, Hakodate 041-0836 Japan.*

Abstract

When phenanthrene (a heavy oil fraction) is subjected to high pressure and heat in a reactor with a metal catalyzer, it produces a markedly anomalous reaction. It produces excess heat and weak radiation, specifically x-rays and gamma-rays. Furthermore, after the reaction finishes, mass spectroscopy reveals what appears to be ^{13}C. It is very difficult to explain the total energy generation as a conventional chemical reaction. After the experiment, almost all phenanthrene and hydrogen gas remains in the same condition they were initially. There are few reaction products such as other chemical compounds. However, the formation enthalpies for these compounds are all negative. The heat generation sometimes reaches 0.1 kW and has continued for several hours. There is a reasonably significant correspondence between the heat generation and the gamma emission. We have confirmed the same result with high reproducibility by controlling temperature and pressure.

1. Introduction

In 1989, Fleischmann and Pons [(1)] reported that palladium electrolyzed in heavy water produces the anomalous heat generation reaction (the cold fusion reaction). Reproducibility and control of the reaction have been difficult, and although many researchers attempted to replicate, most failed. If we assume the reaction is some form of a normal d-d reaction, there should be a much higher neutron flux. However, there are few reports of the neutron observations [(2-8)]. The authors have examined many of the reports of neutrons and have reached the following conclusions:

- First, neutrons and excess heat are rarely observed, but when they are observed, they occur suddenly after electrolysis or discharge have continued for a long time.
- Second, many instances have been reported in which these effects began when some triggering reaction occurred.
- Third, almost all cold fusion experiments have been performed by absorbing the deuterium into the reaction system at first; the electrolyte contains almost pure deuterium gas.

Based on these considerations, we conclude that the cold fusion reaction must be something quite different from conventional d-d fusion. Furthermore, the reaction must involve factors other than absorption of deuterium. After electrolysis has continued for a long time and the deuterium has been replenished, some trigger is likely to occur. We predict that certain triggers are needed to give rise to the reaction.

Many people have asserted that if nuclear reactions are induced by electrochemical reactions using solid electrodes there should also appear clear evidence of the generation of radioisotopes and radiation. Moreover, the evolution rates of reaction products should be quantitatively explained in terms of well-established nuclear reaction mechanisms. These expectations would be valid only if the reaction mechanism is in accord with accepted nuclear theory. There is little reason to believe that is the case.

Mizuno[9], Miley[10], Ohmori[11], Iwamura[12] and others have reported anomalous production of radiation-less foreign elements (Fe, Cr, Ti, Ca, Cu, Zn, Si and so on) on cathode metals (mainly Pd) with heavy water or light water electrolysis experiments. These elements sometimes have drastically non-natural isotopic ratios. These reports present evidence that a nuclear reaction takes place during electrolysis that produces isotopically changed elements on the cathode surface. These elements are generated by a mechanism that does not induce any detectable radiation. The anomalous isotopic abundances of these elements show that they do not come from contamination. Again, the operative nuclear mechanism appears to be completely different from any known nuclear reaction. Whatever it is, if it can be controlled, it appears likely to probably produce tremendous amounts of energy.

The hydrogenation of hydrocarbons has been studied for decades. Song et al.[13] examined the hydrogenation reaction of naphthalene using zeorite supported Pd and Pt catalysts at low temperatures. In particular, they investigated the effect of the catalyst poisoned by sulfur. Fedorynska et al.[14] studied the H_2 transfer reaction between phenanthrene and H_2 in the presence of K/MgO from 250°C to 350°C. Durland et al.[15] tested the hydrogenation of phenanthrene by Raney Ni and CuCrO from 370 K to 573 K. Burger et al.[16] performed pioneering work of the hydrogenation of phenanthrene at ~227°C under 136 to 218 atm of hydrogen gas, which is considered high pressure by the standards of this field. Qian et al.[17] used an alumina supported Pt and Pd catalyst for the hydrogenation of phenanthrene, and they obtained a very high conversion rate, up to 100%. Mahdavi et al.[18-21] and Menini at. al.[22] developed another technique of electrocatalytic hydrogenation that showed a comparably high conversion rate. This study was stimulated by Soejima's research circa 1930 into methods of changing coal to oil by a liquefying reaction. Soejima observed abnormal heat generation during hydrogenation of creosote oil heated in high pressure hydrogen gas. The heat generated was larger than the largest estimated chemical reaction that can occur with few drop of creosote and a little hydrogen gas. Soejima concluded that it could not have come from a conventional chemical reaction.

2. Experimental

2.1 reaction cell

Figure 1 shows a photograph of the two reaction cells used in this study, and experimental setup. The reactors are the cylinders shown in the left side of Fig. 1. The large one is made from Inconel 625. It has a 56 mm outer diameter, 26 mm inner diameter, 160 mm height and the volume is 0.1 L. The smaller one is made from SUS316L, with a 15 mm outer diameter, 9 mm inner diameter and 300 mm height with 0.02 L capacity. The Inconel cylinder can sustain 500 atm of pressure, while the SUS cylinder is limited to less than 200 atm. Both can be heated up to 850°C.

Each cylinder has a hydrogen inlet, gas outlet, and housing for a thermocouple used to measure the internal cell temperature. The cylinder is placed in an electric furnace. A thermocouple to measure the temperature of the outside wall of the reactor cylinder is inserted between the reactor wall and the inner wall of the heater.

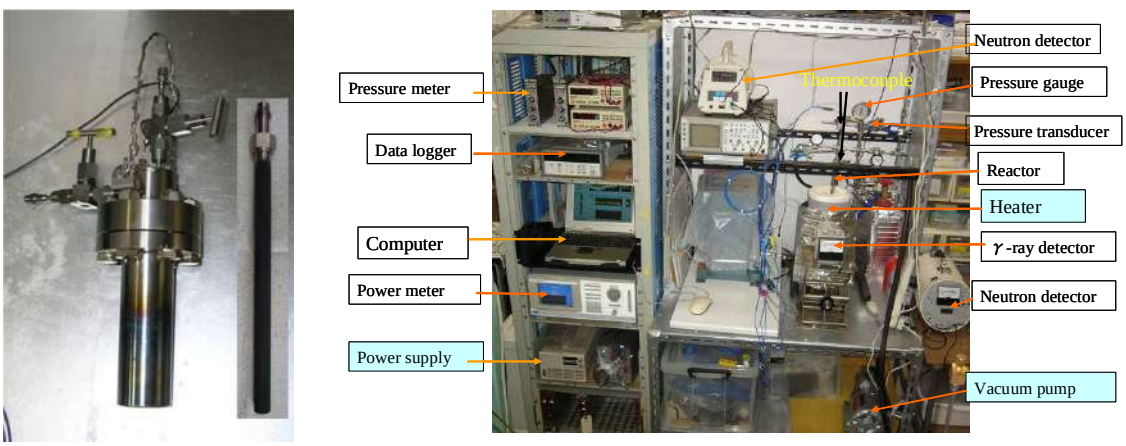

Figure 1. Cell and experimental setup.

2.2 Measurement system

Figure 2 shows a schematic drawing of the measurement setup. The reaction cylinder placed in the heater is shown in gray. An electric power supply is shown in the bottom right, connected to a data logger and recorder.

After the metal catalyzer is put in the reaction container, a few grams of phenanthrene are placed in the cell, and the cover is bolted tightly shut. The reactor is then evacuated to 10^{-3} mmHg. Hydrogen gas is supplied from the gas cylinder up to a constant pressure through a pressure regulator. The electric furnace (Tokyo Technical Lab.: PH, Mo13763A1) was supplied by a 2 kW of power supply. The temperature inside the reactor and the temperature between the reactor and the furnace are continuously measured by R-type thermocouples.

Gamma-ray emission was detected by a detector (Aloka TCS-161) set 15 cm from the reactor, and continuously recorded by a digital multi-meter (Advantest, TR-6845). Temperatures of the heater wire, in the reactor, out of the reactor wall, surface of the gamma detector, and the room were also recorded in the computer through the multimeter.

The mass spectrometer used in this study (ULVAC REGA201) can detect mass numbers up to 400.

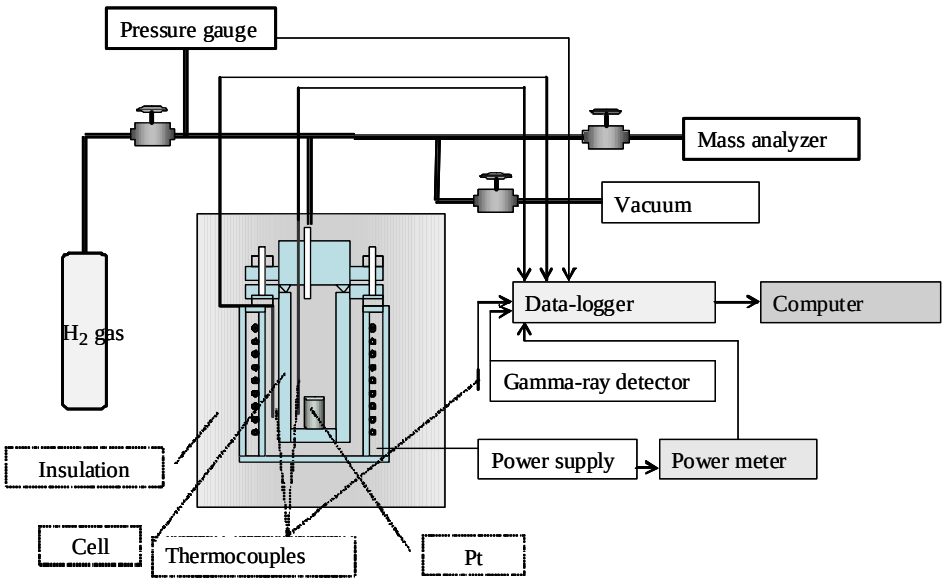

Figure 2. Schematic drawing of the measurement setup.

2.3 Experimental procedures

The fluorescent grade (99.5%) of phenanthrene was supplied by Kanto Chemical Co. LTD. The Pt catalyzer was a high purity Pt mesh (99.99%) supplied by Tanaka Noble Metal Co. LTD. It is rectangular, 5 cm ×10 cm, 50 g. At the beginning of this series of experiments, the Pt catalyzer was activated once in an atmosphere of hydrogen gas for 100 ks at 850°C. When the Pt catalyzer was inactive, it was prepared by oxidizing it in air with an electric heater at 850°C for one hour. As noted, 1 g of phenanthrene and the Pt catalyzer were put in the reactor; the reactor lid was bolted shut. The reactor was connected to the vacuum system and pumped out. The exhaust valve was left open for several minutes to remove residual air. Then the exhaust valve was closed, and hydrogen gas was supplied. The reactor was then heated.

Calibrations for temperature and radiation emission were performed by changing the hydrogen gas pressure from vacuum to 80 atmospheres. The gamma detectors were calibrated by a 3.7×10^5 Bq source of ^{226}Ra that was set at various distances from the detectors, and in the reactor cylinder. The background level of the surroundings was 0.05±0.008 μSv/h.

3. Results

3.1 temperature calibration

We can estimate the anomalous heat caused from the calibration curve obtained from the relationship between input power and the stable temperature of the reactor cylinder.

Figure 3 shows a calibration with the Inconel cell. In this case, a platinum catalyst was placed in the cell, and hydrogen pressure was raised to 50 atm, but there was no phenanthrene in the

cell. The heater was turned on and set to 65 W, and the temperatures at the heater, the cell wall and inside the cell were measured, along with the cell gas pressure. When the heater was turned on, heater temperature rose rapidly at first, followed by the temperature at the cell wall and, after a lag, the temperature inside the cell. After 10 ks the temperature inside the cell drew even with the temperature at the cell wall, and after that the two remained the same as they continued to increase. The cell temperature was never higher than the cell wall temperature. After 15 ks both temperatures reached the same, stable value. In the example shown here, the final temperature inside the cell, at the cell wall and at the heater were all 140°C hotter than the ambient room temperature. The final temperature depends upon various factors such as the heater power, hydrogen pressure, whether or not the phenanthrene or the catalyst are present in the cell, and the size and type of cell selected.

Figure 4 shows the relationship between input power of the heater and the temperature in the reactors. The data was taken under varying conditions of pressure and temperature, with phenanthrene and an inactivated metal catalyzer. Each point represents the final stable temperature achieved when a power setting is maintained; that is, the temperature difference between the reactor and the room. The cell takes about 5 ks (83 minutes) to reach the set temperature with constant input power. The graph shows log-log relationship between the input and the temperature at various hydrogen pressures. The relationship varies with hydrogen gas pressure. The heat conductivity for the gas is nearly constant over a wide range of pressure, from 10^{-3} atm to 10 atm. However, the stable temperatures for each input are decreased at high pressure of H_2, indicating that the gas conductivity increases at more than 10 atm.

The calibration curve derived for the Inconel reactor showed a similar relationship, with the same slope but ten times different input power per degree of temperature. The heat release caused by gas in the reactor is not significant with the Inconel reactor: the temperature deviation stays within ±3°C while the hydrogen gas pressure increased from 1 to 100 atm. Because the Inconel reactor height is 160 mm, the walls of the reactor fit inside the heater envelope (which is 220 mm deep), although the top surface is exposed to air. The SUS reactor has a small diameter and it is longer; 300 mm, so the top 80 mm of the reactor walls protrudes. Some heat release from the exposed portions of the reactors occurs.

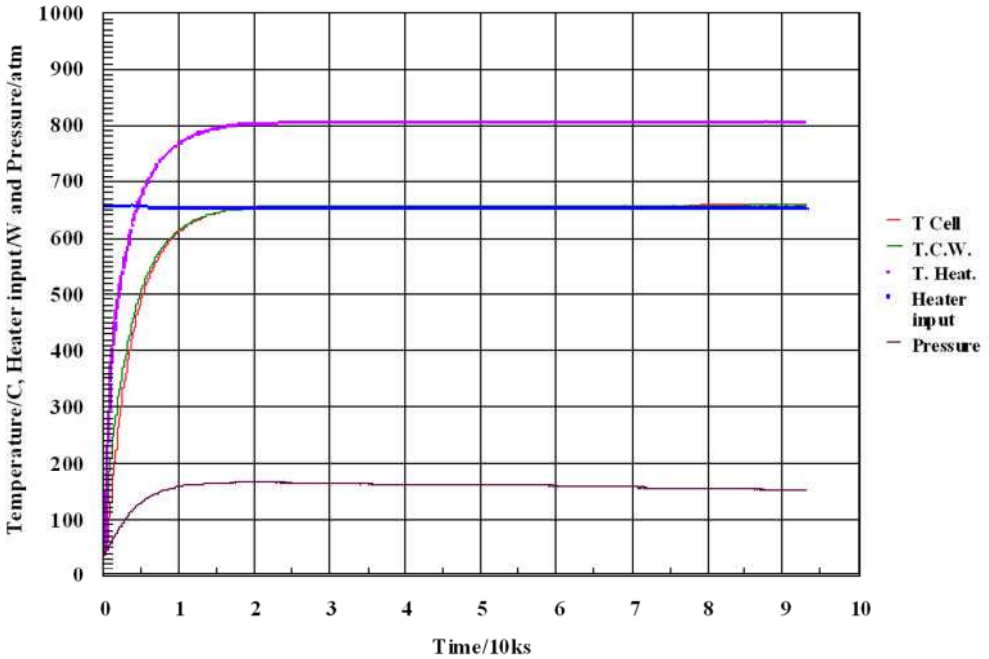

Figure 3. Temperature, pressure and heater power with the Inconel reactor at 650 W input and H_2 at 50 atm with no phenanthrene sample. Three temperatures are measured in this test: inside the cell (T cell) at the cell wall (T.C.W), and at the heater (T. Heat.).

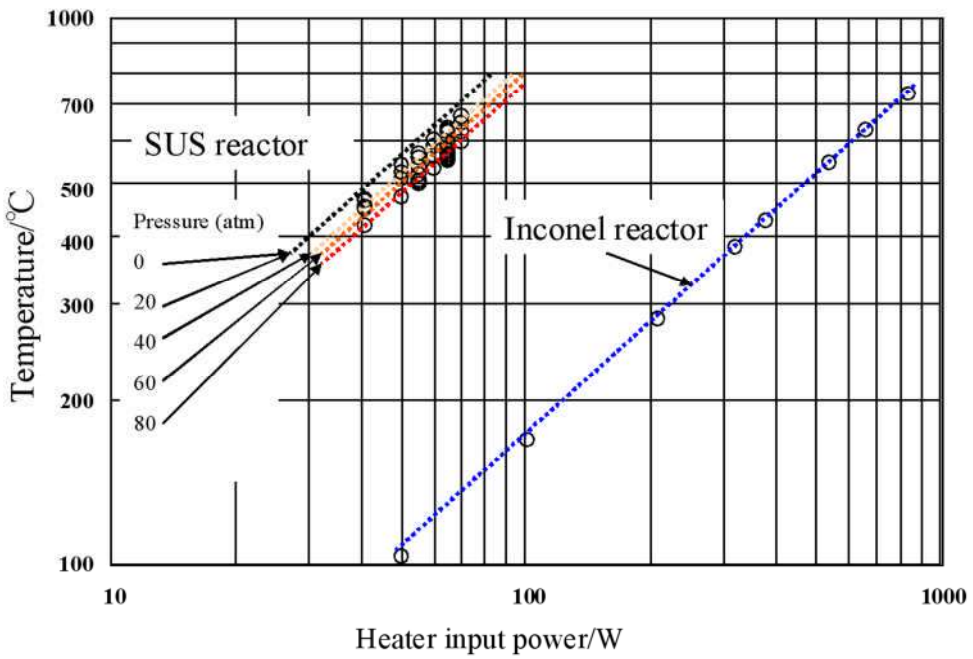

Figure 4. Heater input dependence of reactor temperature at various H_2 pressure settings.

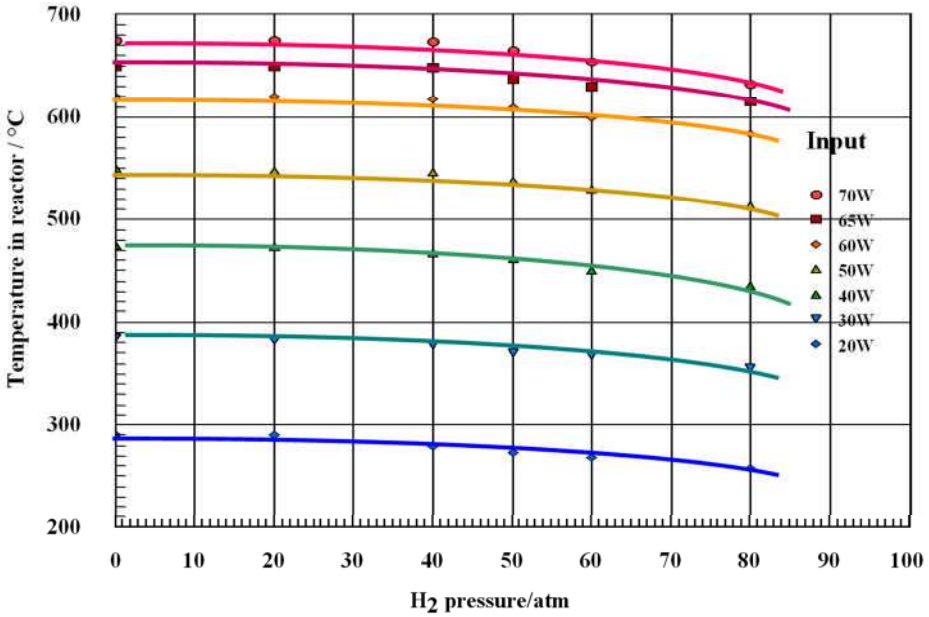

Figure 5. H_2 pressure dependence of reactor temperature at various input power.

The relationship between temperature (T) and input heat (W) is represented by a simple equation $T = CW^k$ in the temperature region of this experiment. The constant of the exponent k for the relationship is nearly the same for all the calibration conditions, at 0.6. The heat conductivity of hydrogen is 0.18 W to 0.42 W m^{-1} K^{-1} from 373 K to 1273 K and is almost constant at the pressure range from 1 to 100 atm [23, 24]. However, heat conductivity of the gas increases at the high pressure range, as indicated in Fig. 4. The heat release radiation is described by the equation below. This is non-linear. The coefficient k is 0.6 because the process of heat release depends on conductivity and radiation. Conductivity increases with temperature. The heat release also depends on the radiant process at high temperature region:

$$P = \sigma \varepsilon A(T_s^4 - T_a^4)$$

Here, P is heat release (W m^{-1} K^{-1}), σ is Stefan-Boltzmann constant (5.67×10^{-8} W m^{-2} K^{-4}), ε is the radiant constant, T_s is absolute temperature of the body and T_a is ambient room temperature. With both the Inconel and SUS cells, the area above the heater exposed to air is roughly 30 cm^2. The radiation rate from a metal surface is about 0.9. In this experiment, the highest temperature achieved is 700°C, or 1000 K. According to the above equation, at this temperature the exposed metal surface radiates 40 W. At 500 K, it would radiate 10 W, and at 300 K 1.4 W. This heat loss amounts to a rate of around 50% with the small SUS cell, and 10% with the Inconel cell. The heat loss rate grows larger as the temperature rises. Figure 3 shows that with the SUS cell above 600°C the calibration curve peak is reduced. But with the Inconel cell, even above 700°C no significant heat loss to radiation is observed.

If anomalous heat is generated, the calibration will clearly show that this occurred.

3.2 Gamma ray calibration

Figure 6 shows background gamma activity, and the intensity spectrum for the gamma activity is shown in Fig. 7. The background is steady at 0.05 μSv/h, in a Poisson distribution, as shown in the blue line.

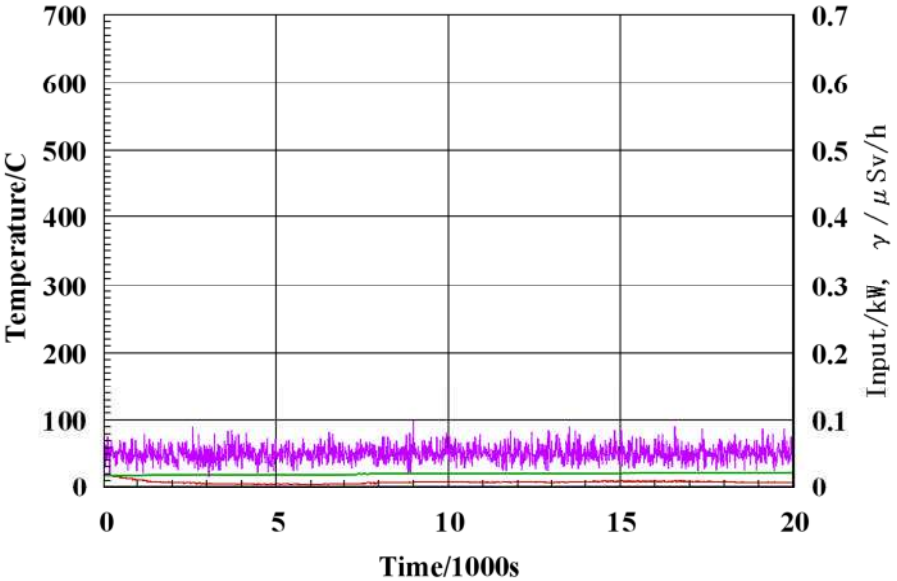

Figure 6. Background gamma emission.

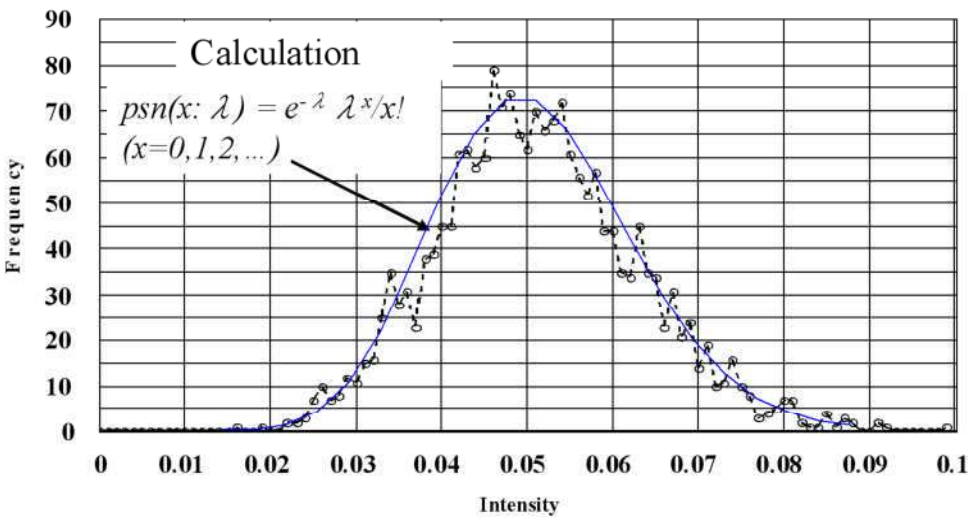

Figure 7. Intensity spectrum for background gamma emission.

Figure 8 shows gamma emission change with 0.1μCi (= 3.8 kBq) of Ra-226. This graph shows data over 1.57 ks, with the gamma source placed 10 cm from the detector. The source was first placed near the detector at 1.8 ks, and removed at 4 ks. The times before and after this show the background gamma ray levels.

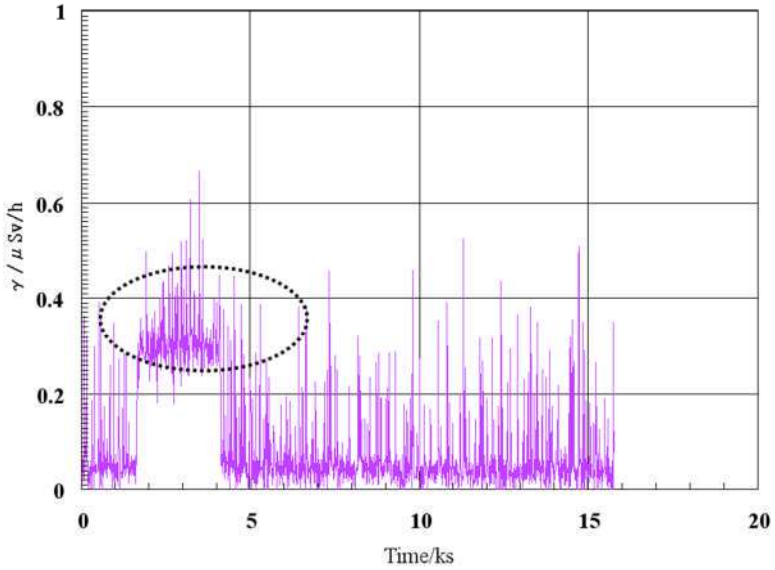

Figure 8. A calibration with Ra-226 placed 10 cm from the cell. Data from the Geiger counter.

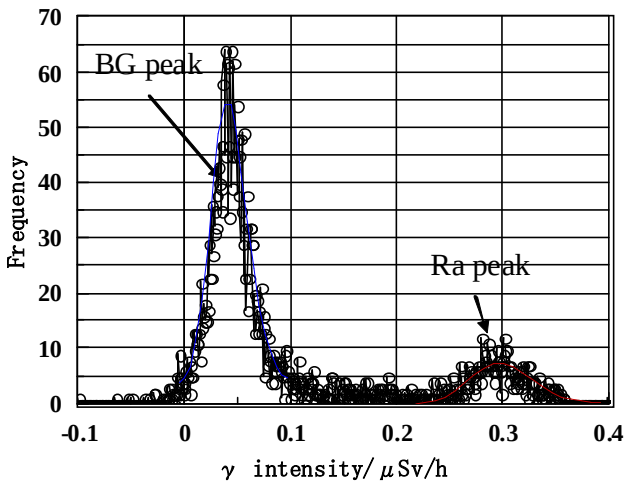

Figure 9. Intensity spectrum for gamma emission during calibration with Ra-226. Data from the ionization chamber.

Figure 9 shows the intensity distribution of gamma emission of Fig. 8. Two peaks are shown in the intensity distribution: at 0.05 μSv/h from the background; and at 0.3 μSv/h from a gamma source. The solid red line shows the computed distribution. In this example, the gamma peak is pronounced and easy to separate from the background, but when the Ra-226 gamma source is farther from the detector, or when it is left in place for a shorter time, the separation is not clear.

Figure 10 shows a calibration with the gamma source placed 10 cm from the detector for 1.2 ks. This produces an extra peak above the 0.22 μSv/h background peak. Figure 11 shows a

calibration with the gamma source placed 30 cm from the detector. A weak peak of 0.04 μSv/h can be seen.

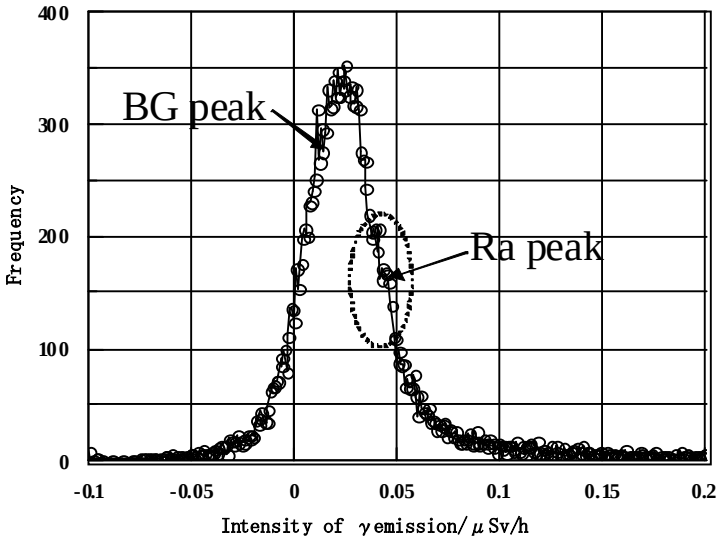

Figure 10. Calibration with gamma source 10 cm from detector

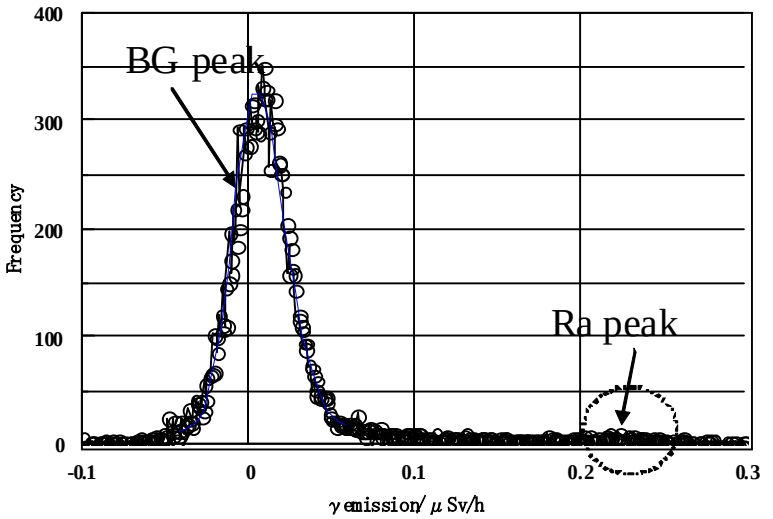

Figure 11. Calibration with gamma source 30 cm from detector

3.3 control experiments

The following control experiments have been performed:

- Hydrogen gas, and a platinum mesh, but no phenanthrene.
- Helium gas, a platinum mesh, and phenanthrene.
- Vacuum only; no gas.

These tests did not produce measureable anomalous heat, gamma rays or a change in mass 13.

4. Results

4.1 Excess heat generation

Figure 12 shows an example of anomalous excess heat. In this test, 1 g of phenanthrene was exposed to a mixture of 1 atm of hydrogen and 70 atm of helium gas. Heater power is initially set for 1.4 kW, then after 3 ks it is reduced to 700 W. Finally, it is reduced to 640 W. The heater temperature (T_2) rises faster than the cell temperature (T_1). At 10 ks they both stabilize at around 640°C, which is where the calibration curve (Fig. 4) predicts they will settle if there is no anomalous heat. However, they both soon begin to rise above the calibration point. Figure 13 is a magnification of Fig. 12 at the peak of heat production. At 9 ks the cell temperature T_1 stabilizes for about 2 ks as the heater temperature continues to rise. The cell temperature begins rising again and at 12 ks it exceeds the heater temperature T_2. This temperature reversal is definitive proof that heat is being produced inside the cell. When power is turned off, at 16 ks, the heater temperature T_2 peaks at 670°C and the cell temperature T_1 has reached 690°C (20°C higher than T_2). Input heater power is 640 W. The cell wall temperature at T_2 peaks at 670°C which is only as high as the calibrated point for this power level; unlike T_1, it does not indicate any excess heat.

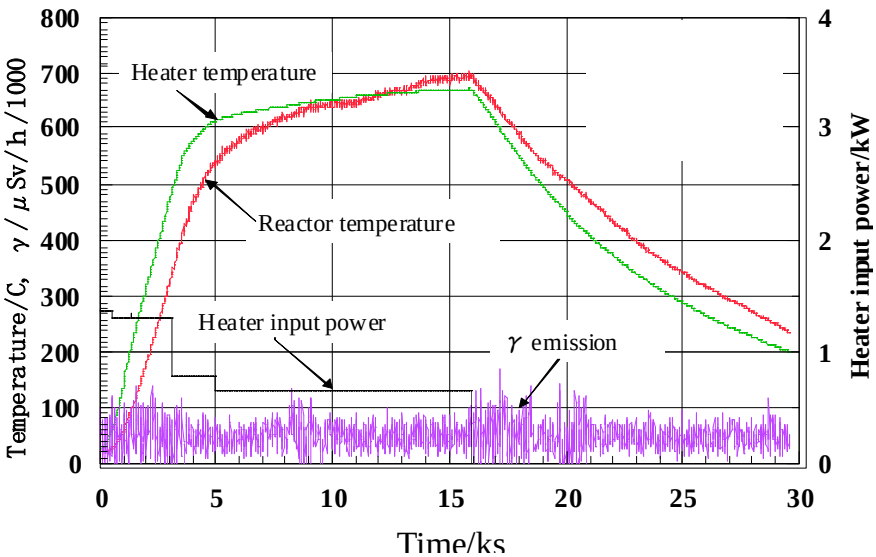

Figure 12. An example of anomalous excess heat.

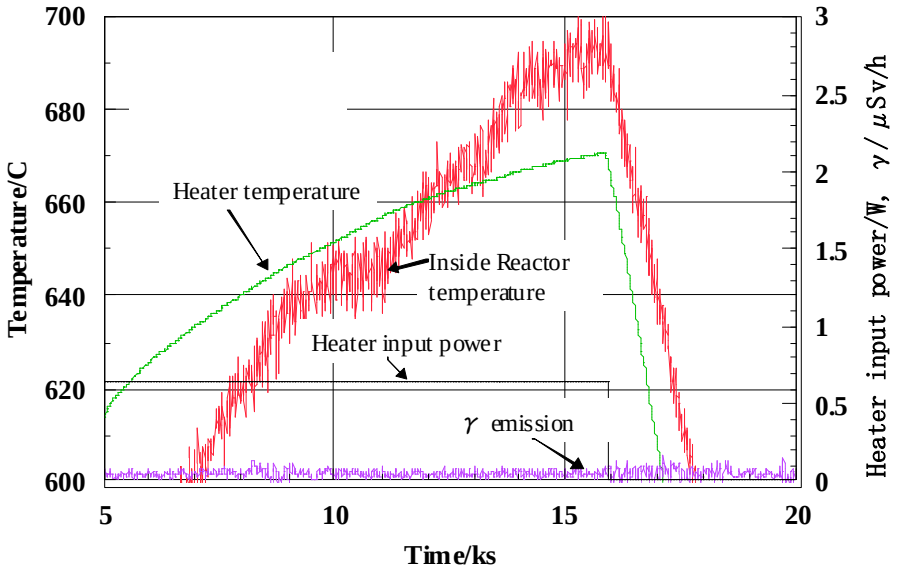

Figure 13. Magnification of Figure 7 data at peak of anomalous power output.

Total energy is more difficult to estimate than power, but given that the excess power persisted for 6 ks (100 min.) it was at least 120 kJ, for this test. Other tests have produced more energy.

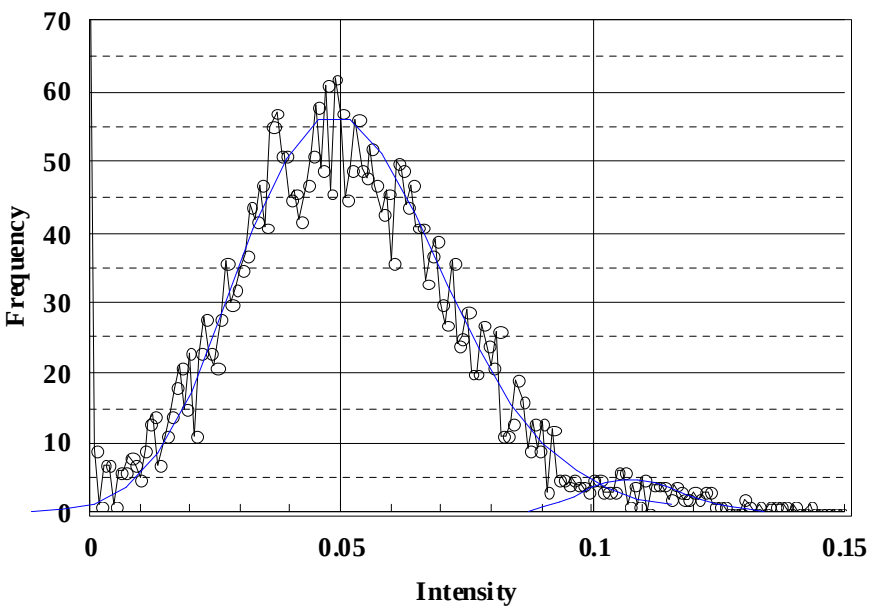

Figure 14. Intensity spectrum for the foreground gamma emission in Figure 11.

Figure 14 shows the energy intensity spectrum from the ionization chamber gamma detector. After mathematical treatment it is clear that a 0.11 μSv/h peak is superimposed on the 0.05

μSv/h background. Similar large gamma peaks are rare but they have been observed during high excess heat production.

Figure 15 shows another example of anomalous heat production. In the first stage, 1 atm of hydrogen and 70 atm of helium are admitted into the cell, and the temperature is raised to 680°C. After 10 ks, the temperature reaches the calibrated point. After that the temperature inside the cell goes well above this point. At 60 ks in this graph, it goes above 700°C, 20°C above the calibration.

At 74 ks the heater power is lowered, but the cell temperature actually rises abruptly. Later, as the temperature fall, the cell temperature fluctuates a great deal.

During this time, gamma ray activity is much larger than background, especially when intense heat is generated.

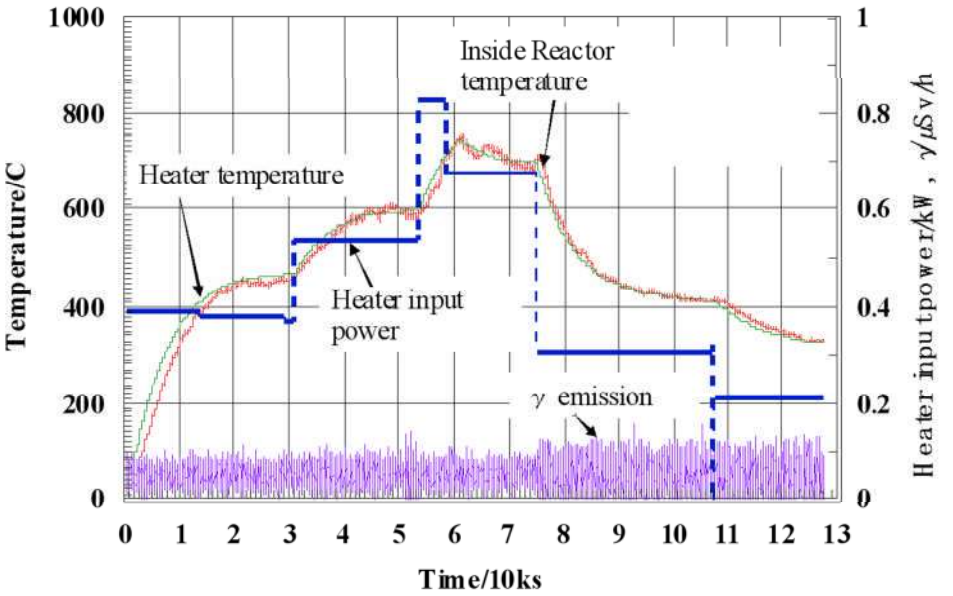

Figure 15. Anomalous heat production, example 2.

Figure 16 shows the calculated and measured intensity distributions for the gamma-ray emission detected with the ionization chamber. There are three peaks: two in the foreground data at 0.07 and 0.11 μSv/h, and another of the background at 0.05 μSv/h. All have a Poisson distribution. In this case, one of the peaks is at 0.11 μSv/h, the same as case shown in Fig. 14. The intensity of the gamma radiation is more than two times that of the background although the peak height of the spectrum is very weak compared with the background.

Figure 17 shows an enlargement of data from the heat generation experiment shown in Fig. 15. The cell temperature begins to rise rapidly at 74.5 ks. At 75 ks, the furnace heater input power is reduced from 700 to 300 W. The furnace heater temperature immediately begins to fall, yet the cell temperature continues to rise. Eventually it rises to 40°C above the previous furnace heater temperature. The only heat being supplied to the system comes from the furnace

heater, so if there is no anomalous heat within the cell, it is thermodynamically impossible for the cell temperature to rise above the furnace heater temperature, and it is also impossible for it to continue to rise as the furnace heater temperature drops.

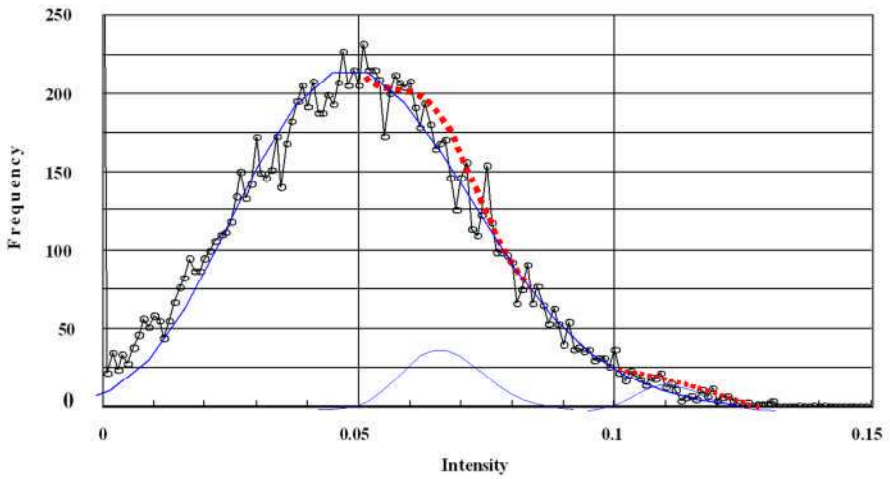

Figure 16. Intensity spectrum for the foreground gamma emission in Figure 15.

With this technique, unlike electrochemical cold fusion, there is no electrolysis power or other direct input power. The only input is to the heater, so once high-temperature triggers a reaction, all of the anomalous heat is self-sustaining. The reaction could be sustained without electricity by insulating the cell to maintain the temperature, but this would make it difficult to control the temperature.

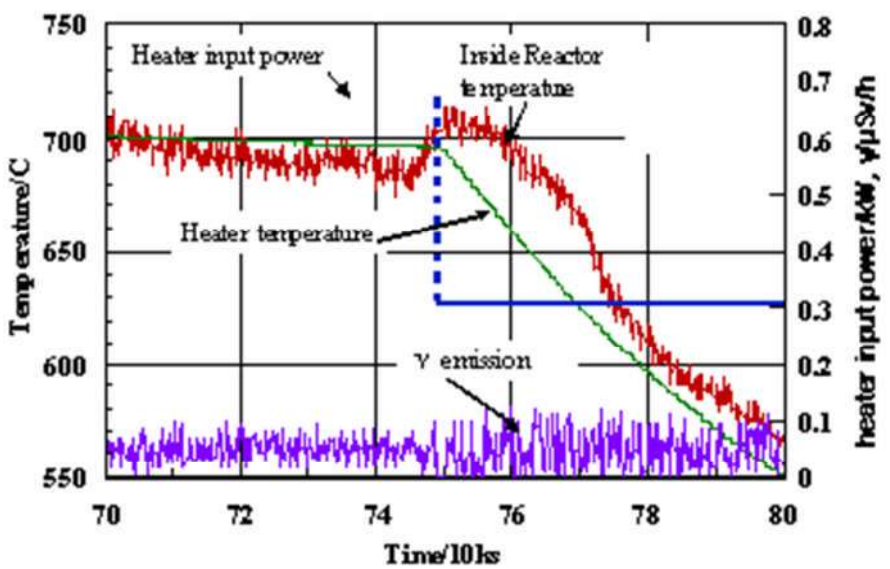

Figure 17. At 75 ks input heating power is lowered, but the cell temperature rises.

4.2 Coincidence between gamma emission and heat generation

As shown above, with the Inconel cell we were able to confirm anomalous heat production. Furthermore, we confirmed that gamma-rays were produced while anomalous heat was produced. However, with the large 0.1 L cell, we are only able to measure heat in part of the cell, and we cannot be sure what part of the cell the heat originates from. Response is slow because the thermal mass of the cell is large. To alleviate this problem, we constructed a smaller cell, and we took other steps to correlate heat production with gamma ray production. The smaller cell is made from the SUS alloy, with 9 mm diameter. The phenanthrene sample and platinum catalyst are placed at the bottom of the cell, and the thermocouple is placed in direct contact with the catalyst, so that temperature changes can be rapidly detected. With this arrangement, gamma-ray emission and changes in temperature can be directly compared.

Figure 18 shows an example of data from the SUS cell. The platinum catalyzer and 1 g of phenanthrene are placed at the bottom of the cell, and 50 atm of hydrogen gas is admitted to the cell. The cell is heated and changes in temperature and gamma ray emission are recorded. Heater power is set at 55 W, so the temperature is expected to reach 595°C according to the calibration. The figure shows data between 30 and 82 ks. The temperature reaches 595°C as expected, and then gradually exceeds it. Furthermore, when this happens, the temperature inside the cell (the red line) rises before the temperature at the cell wall (green line). Note that both of these temperatures are below the heater temperature, which is 700°C, and not shown in this graph. Note also that the temperature fluctuations inside the cell are large. Detailed data from the right portion of this graph is shown below, in Fig. 19.

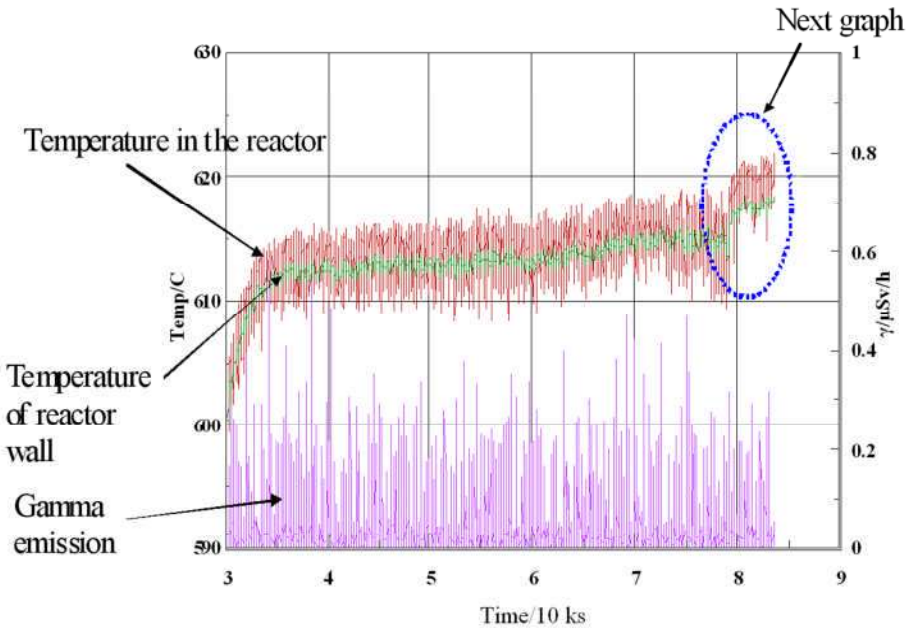

Figure 18. Change in temperature and gamma emission during hydrogenation.

Figure 19 shows high resolution data, with individual data points taken at 5-second intervals. The purple line indicates gamma rays. It can be seen that immediately after gamma ray bursts,

the temperature rises. Especially after a large gamma ray burst, a corresponding temperature rise can be seen. Many other examples of this have been observed. In this case, the calibrated temperature for the heater input is 600°C but the cell temperature rapidly and repeatedly rises to 620°C before returning to the equilibrium temperature of 600°C.

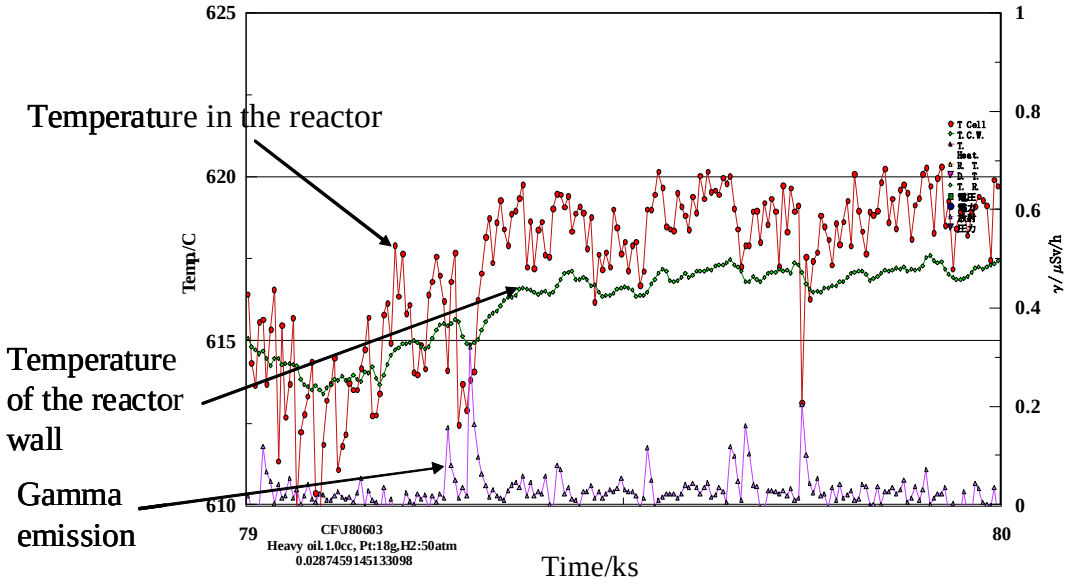

Figure 19. Gamma activity at the onset of anomalous heat.

4.3 Mass analysis after experiment

Figure 20 shows the normalized mass spectra for five runs with different starting conditions and outcomes. The red points show the gas after excess heat generated. The other colors show the gas after various null experiments, In these tests, the phenanthrene sample (when present) is 1 g; the platinum catalyst is 27.8 g; hydrogen is at 54 atm, the temperature was held at 600°C for 10 days. The M/e numbers were measured up to 100.

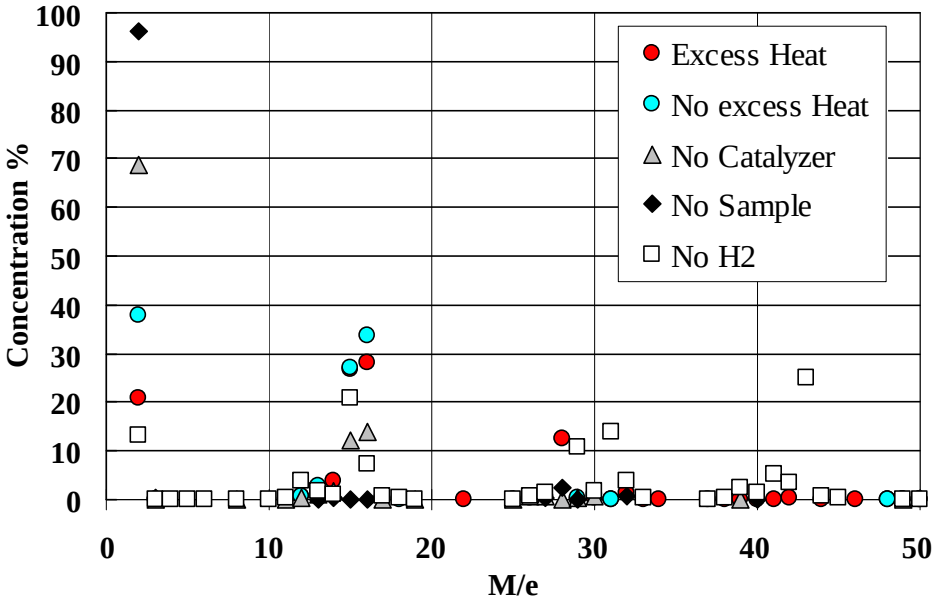

Figure 20. Mass spectrum of gas sample taken after the experiment.

The values in this graph were computed by the following method:

(1) The value was normalized to the pressure measured during the test.

(2) Background values for the elements already present in the cell are measured at the time the gas was admitted to the cell, and subtracted from the values measured after the experiment.

(3) The species with the highest concentration was H_2^+ which was 96.2% of the gas in the test with no phenanthrene present. This is shown as the black diamond on the top right.

The symbols in Fig. 20 are described in Table 1. This shows, for example, that the red circles (data taken when excess heat was produced) represent different species. The red circle at mass number 2 (M/e 2 on X-axis) indicates H_2^+ which is 21% of the total. The red circle at mass number 12 represents C^+, which is 0.7% of the total mass of the sample.

Table 1. Cell conditions for the five runs shown in Fig. 20.

Symbol, meaning	Cell conditions		
	Pressure	Temperature	Gas volume
● Excess heat produced	37 atm	650°C	0.33 L
● No excess heat	60 atm	605°C	0.56 L
▲ No catalyzer in cell	54 atm	645°C	0.48 L
♦ No sample phenanthrene in cell	38 atm	660°C	0.33 L
□ No H_2 gas in cell	0.33 atm	350°C	0.004 L

Table 2. Percent of each species found for the five runs shown in Fig. 20.

Mass number	Species	Percent of all gas				
		● Excess heat produced	● No excess heat	▲ No catalyzer in cell	♦ No sample phenanthrene in cell	□ No H_2 gas in cell
2	H_2^+	21	37	68	96.2	13
12	C^+	0.7	0.7	0.3	0	3.7
13	$^{13}C^+$	2.5	2.6	1.0	0	1.8
14	CH_2^+	3.8	1.0	1.6	0.36	1.1
15	CH_3^+	27	27	12	0	21
16	CH_4^+	28	34	12	0.1	7.5
17	OH	0.3	0	0.1	0	0.8
28	N_2	12.5	0	0.1	0.25	0
29	C_2H_5	—	—	—	—	11
43	C_3H_7	—	—	—	—	25

Based on the analysis of the gas, in all four tests with the sample phenanthrene present in the cell, hydrocarbon species were found, including C1 species (CH_2, CH_3, CH_4), C_2 (C_2H_3, C_2H_4), and C_3 (C_3H_3, C_3H4, C_3H_5, C_3H_6, C_3H_7).

The above analysis is for the relative amounts of gas, not the absolute amounts. The actual amount of gas present in the cell varies with gas pressure and temperature. Total cell volume is 0.03 L, but the equipment in the cell such as the catalyst take up 0.01 L, leaving 0.02 L free space for the gas. After taking into consideration the gas pressure and temperature, the total gas volume of $^{13}C^+$ at STP for the 5 tests is estimated as follows:

- ● Excess heat produced, 8.25 ml
- ● No excess heat, 14.6 ml
- ▲ No catalyzer in cell, 4.8 ml
- ♦ No sample phenanthrene in cell, 0 ml
- □ No H_2 gas in cell, 0.0072 ml

ICP mass spectroscopy (Finnigan Mat Element: outsourced) was performed, with the following parameter settings. ICP settings: high frequency 27 MH, 2.0 kW, earth potential; analyzer: double-focus; mass range: 5 – 260; mass resolution, variable: 300, 3000 or 7500; slit: variable resolution; analysis acceleration voltage: 8 kV; magnetic field radius: 16 cm; electric field orbital radius 10.5 cm; detector: dual mode SEM – analog/ion counter; detection limit 0.1 ppt; internal standard calibration element: ^{115}In. Current measurement or ion counting uses an electron multiplier.

Solids found in the cell after the reaction were analyzed. Before the experiment, the carbon in the cell was 99% ^{12}C, but after heat was produced in the example shown in Fig. 20, more than 50% of the carbon in the phenanthrene sample was $^{13}C^+$.

The largest mass of carbon products from the reaction were found after the experiment shown in Fig. 18 in which no excess heat was found (●). This was followed by:

● Excess heat produced, with all necessary elements in the cell; the catalyzer, phenanthrene and gas.

▲ No catalyzer in cell

□ No H_2 gas in cell, no reaction

♦ No sample phenanthrene in cell, no reaction

In the test that produced no heat, and the test with no catalyst, $^{13}C^{+}$ was detected. There does not appear to be a correlation between the amount of heat produced and the amount of $^{13}C^{+}$. Also, in tests without the catalyst, it is possible that the nickel in the cell wall alloy may act as a catalyst for the reaction.

5. Discussion

We used only 1 g of phenanthrene as the reactant. We have checked the weight of phenanthrene in the reactor after the experiment. Due to the high temperature of the experiment, a portion of the reactant evaporated and was adhered on the reactor inner surface and on the Pt catalyzer. This reactant was collected by wiping it off with filter paper. The phenanthrene recovered from the cell weighed 0.99 g; the reactant weight decreased by 0.01g. However, it was difficult to weigh the loss of the reactant exactly, because it was impossible to completely recover the reactant.

The addition of hydrogen to a carbon-carbon double bond is called hydrogenation. The overall effect of such an addition is the reductive removal of the double bond functional group. Although the overall hydrogenation reaction is exothermic, high activation energy prevents it from taking place under normal conditions. This restriction may be circumvented by the use of a catalyst, such as Pt.

Catalysts act by lowering the activation energy of reactions, but they do not change the relative potential energy of the reactants and products. Finely divided metals, such as platinum, palladium and nickel, are among the most widely used hydrogenation catalysts.

Usually the reaction of hydrogenation of carbon hydride is exothermic, and heat is released corresponding to the ΔE. For example, ΔE is around -125 kJ/mole. Another case, for example, hydrogenation reaction for benzene is:

$$C_6H_6 + 3H_2 = C_6H_{12},\ \Delta H = -207\ \text{kJ/mol-benzene}$$

But the enthalpy of the hydrogenation reaction of phenanthrene is different depending on the temperature. It is a reaction of heat generation less than 300°C [25]. However, it is an endothermic reaction consuming kilojoules per mole at temperatures higher than 300°C. We observed that less than 0.01 g of phenanthrene reacted with the high pressure H_2 gas. So, the molar value of the reactant phenanthrene was only 5.6×10^{-5}. Thus, the heat of the reaction can be estimated as 11.2 J. Total heat observed during the experiment was on the order of 10^2 kJ,

10^4 times higher than a chemical reaction would allow. Therefore, a chemical reaction is ruled out.

The amount of anomalous heat was lower than with hydrogen alone than it was with hydrogen mixed with helium. Hydrogen is a significant constituent in phenanthrene, so it seems likely that this constituent hydrogen was involved in the reaction.

A weak gamma line discharge is observed during the experiment. This indicates that some sort of nuclear reaction occurred, although the correlation of the heat generation and this gamma line radiation was low. The gamma emission increased somewhat on average when anomalous heat was generated, occasionally to levels several times background, but not dramatically. The gamma emission was sporadic, which may indicate that the reaction causing the gamma emission and the heat occurs in very short time.

6. Conclusions

The anomalous energy generation cannot be the product of a conventional chemical reaction for the following reasons:

- At these temperatures, hydrogenation reactions are endothermic, not exothermic.
- The total heat release far exceeded any known chemical reaction with this mass of reactants.
- There is virtually no chemical fuel in the cell.
- There were no chemical reaction products. The components and chemical species in the cell including phenanthrene and hydrogen gas remained essentially as they were when experiment began, except that the platinum screen was coated with carbon.
- Gamma emissions are characteristic of a nuclear reaction.

The reaction is reliably triggered by raising temperatures above the threshold temperature of ~600°C and the hydrogen pressures above 70 atm. It can be quenched by lowering the temperature inside the cell below ~600°C.

When the necessary conditions are achieved, generation of heat is observed with high reproducibility. However, the amount of heat generated is not stable. Only a small amount of reactant is consumed during the experiment, presumably by conventional chemical reactions. We conclude the following:

1. Anomalous heat generation was confirmed during heating of phenanthrene in high pressure of H_2 gas.
2. Sporadic gamma emission was confirmed during high temperature experiment.
3. A weak correlation was observed between heat and gamma ray emissions.

Acknowledgements

We thank Brian Scanlan of Kiva Labs for support.

References

1. M. Fleischmann and S. Pons: J. Electroanal. Chem. 261 (1989) 301.
2. Chicea, D. and D. Lupu, *Low-intensity neutron emission from TiDx samples under nonequilibrium conditions.* Fusion Technol., 2001. **39**: p. 108.
3. Choi, E., H. Ejiri, and H. Ohsumi, *Application of a Ge detector to search for fast neutrons from DD fusion in deuterized Pd.* Jpn. J. Appl. Phys. A, 1993. **32A**: p. 3964.
4. Mizuno, T., et al., *Neutron Evolution from a Palladium Electrode by Alternate Absorption Treatment of Deuterium and Hydrogen.* Jpn. J. Appl. Phys. A, 2001. **40**(9A/B): p. L989-L991.
5. Klyuev, V.A., et al., *High-energy Processes Accompanying the Fracture of Solids*. Sov. Tech. Phys. Lett., 1986. 12: p. 551.
6. Dickinson, J.T., et al., *Fracto-emission from deuterated titanium*: *Supporting evidence for a fracto-fusion mechanism*. J. Mater. Res., 1990. 5: p. 109.
7. Preparata, G., *A new look at solid-state fractures, particle emission and 'cold' nuclear fusion*. Nuovo Cimento A, 1991. 104: p. 1259.
8. Fateev, E.G., *Possibilities for establishing the mechanism of neutron generation in deuterated materials under mechanical loading*. Tech. Phys. Lett., 1995. 21(5): p. 373.
9. Tadahiko Mizuno, Tadayoshi Ohmori, Kazuya Kurokawa, Tadashi Akimoto, Masatoshi Kitaichi, Kohichi Inoda, Kazuhisa Azumi, Sigezo Shimokawa and Michio Enyo, "Anomalous isotopic changes for the elements induced by cathodic electrolysis of Pd electrode" Denki Kagaku, **64**, No.11 (1996) 1160-1165 (in Japanese).
10. George H. Miley, and James A. Patterson, "Nuclear transmutations in thin-film nickel coatings undergoing electrolysis" J. New Energy, **1,** No.3 (1996) 5-39.
11. 11 Tadayoshi Ohmori, Tadahiko Mizuno, Yoshinobu Nodasaka and Michio Enyo, "Transmutation in A Gold-Light Water Electrolysis System" Fusion Technology, **33** (1998) 367-382.
12. Y. Iwamura, M. Sakano and T. Itoh, Elemental Analysis of Pd Complexes: Effects of D_2 gas permeation. Jpn. J. Appl. Phys. **41** (2002) 4642-4648.
13. Chunshan Song and Andred D. Schmitz, "Zeolite-Supported Pd and Pt Catalysts for Low-Temperature Hydrogenation of Naphthalene in the Absence and Presence of Benzothiophene" Energy & Fuels, 11(1997) 656-661.
14. Elzbieta Fedorynska and Piotr Winiarek, "Influence of gaseous hydrogen on the hydrogen transfer reaction between phenanthrene and hydrogen donors", Reaction Kinetics and Catalysis Letters 63 (2) (1998) 235-239.
15. John R. Durland and Homer Adkins, "Hydrogenation of Phenanthrene" J. Am. Chem. Soc., 59 (1937) 135-137.
16. Alfred Burger and Erich Mosettig, "Studies in the Phenanthrene Series, XIII. 9,10-Dihydrophenanthrene and Amino Alcohols Derived from It" J. Am. Chem. Soc., 58 (1936) 1857-1860.
17. Weihua. Qian, Yosuke Yoda, Yoshiki Hirai, A. Ishihara and T. Kabe, "Hydrodesulfurization of Dibenzothiophene and hydrogenation of phenanthrene on Alumina-Supported Pt and Pd Catalysts", Appl. Catal., A: General 184 (1999) 81-88.
18. Behzad Mahdavi, Jean Marc Chapuzet and Jean Lessard. "The electrocatalytic

hydrogenation of phenanthrene at Raney nickel electrodes: the effect of periodic current control". Electrochim. Acta 38 (1993) 1377-1380.
19. Behzad Mahdavi, P. Los, M. Jean Lessard and Jean Lessard. "A comparison of nickel boride and Raney nickel electrode activity in the electrocatalytic hydrogenation of phenanthrene". Can. J. Chem. 72 (1994) 2268-2277.
20. Jean Mark Chapuzet, Behzad Mahdavi and Jean Lessard. "The electrocatalytic hydrogenation of phenanthrene at modified Raney nickel electrodes". J. Chim. Phys. 93 (1996) 1252-1261.
21. Behzad Mahdavi, Jean Marc Chapuzet, M. Jean Lessard and Jean Lessard. "Determination of intrinsic electrode activity in the electrocatalytic hydrogenation of phenanthrene". 76th CSC Conference, Sherbrooke, May 30-June 3, 1993.
22. Richard Menini, Anna Martel, Hugues Ménard, Jean Lessard and Olivier Vittori "The electrocatalytic hydrogenation of phenanthrene at Raney nickel electrodes: the influence of an inert gas pressure". Electrochim. Acta, 43 (1998) 1697-1703.
23. "Materials of Engineering of Heat Conductivity" Edited by Japan Society of Mechanical Engineering, pressed by Maruzen, (1986) 337.
24. Ikuji Takagi, Kouhei Toyoda, Masaaki Katayama, Haruyuki Fujita and Kunio Higashi, J. Nucl. Mater. Vol.258-263 (1998) pp.1082-1086.
25. Wendell H. Wiser and Alex G. Oblad "High conversion of coal to transportation fuels for the future with low HC gas production" Progress Report No. 2, (Covering the period January 1 – March 31, 1993) April 1993.